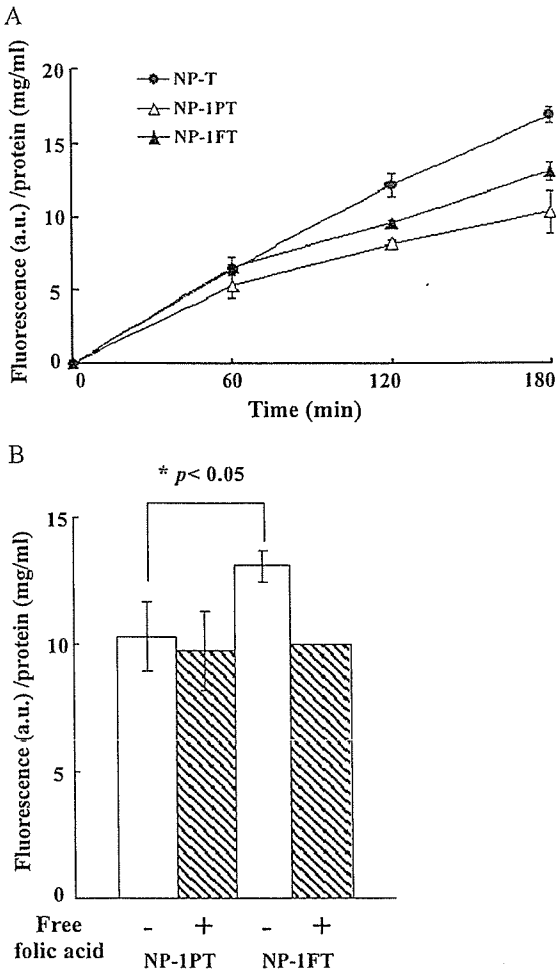

Fig. 2. Association of DiI-labeled nanoplexes with KB cells. In A, NP-T, NP-1PT or NP-1FT were mixed with 4 μg DNA at charge ratio (+/−) of 3/1. The nanoplexes were incubated with KB cells, plated overnight in a 6-well plate at 1×10^5 cells/well, in the presence of 2 ml medium containing 10% serum. After 1, 2 or 3 h, each cell was washed with PBS, detached with 0.25% trypsin from the dish and then centrifuged at 1500 × *g*. The pelleted cells were lysed with PBS containing 0.5% Triton X-100. Associations of DiI-labeled nanoplexes were quantified using a fluorescence plate reader at excitation and emission wavelengths of 550 and 570 nm, respectively. In B, each nanoplex was incubated with KB cells in the absence or presence of 1 mM folic acid for 3 h. Each value in A and B represents the mean ± S.D. ($n=3$). *$P<0.05$ compared with NP-1FT without free folic acid.

was still bound to NP-1FT in some places. These findings shown in Fig. 3E and F were also observed in KB cells (data not shown).

3.7. Luciferase expression in KB and LNCaP cells

We evaluated the transfection efficiency of six kinds of NPs in the presence of 10% serum by luciferase activity. KB or LNCaP cells were transfected using NPs with the plasmid coding luciferase gene for 24 h. NP-1FT showed the highest luciferase activity in the KB cells, and the other NPs showed very low luciferase activities (Fig. 4A). NP-0.3FT and -1FT showed the high luciferase activities in

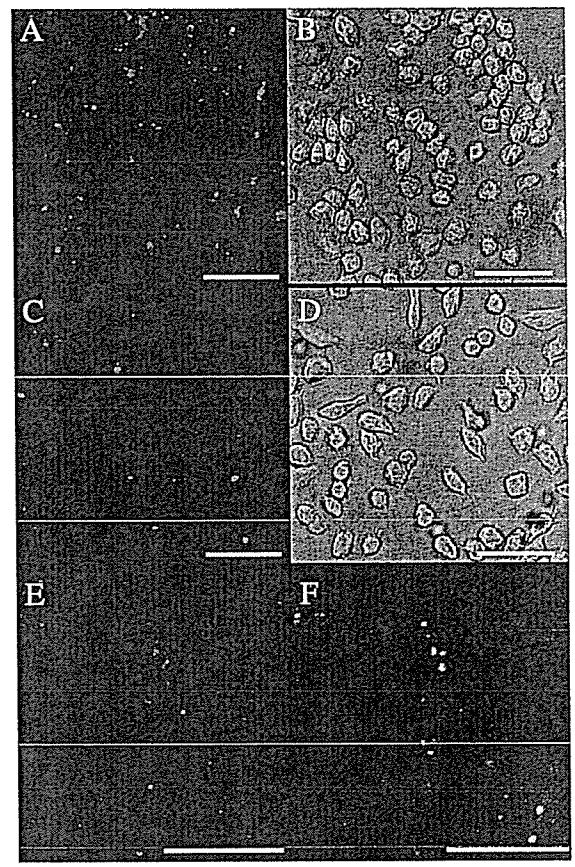

Fig. 3. Selective association of FR-targeted nanoplex with KB and LNCaP cells. KB cells were treated with the nanoplex of NP-1FT in the absence (A and B) or presence (C and D) of 1 mM folic acid for 24 h. In E and F, DiI-labeled NP-1FT was mixed with FITC-labeled DNA, and then incubated with LNCaP cells for 24 h. DiI-labeled NP-1FT and FITC-labeled DNA were visualized by confocal microscopy (magnification × 600 in panels A–D and × 1000 in panels E and F). In panels A–E, red signals show the localization of DiI-labeled NP-1FT, and in panel F, green signal shows that of FITC-labeled DNA. Scale bar = 50 μm.

LNCaP cells (Fig. 4B). Tfx20, a commercial gene transfection reagent, showed about 5-fold higher transfection efficiency in KB cells (1×10^3 cps/μg protein, equivalent with 1.9×10^3 RLU/μg protein) and about 50-fold higher in LNCaP cells (5×10^4 cps/μg protein, equivalent with 1×10^5 RLU/μg protein) than those by NP-1FT (data not shown). NP-1FLT reduced the transfection activity. In NP-0.3FT, the different profile of transfection activities was observed between both cell lines.

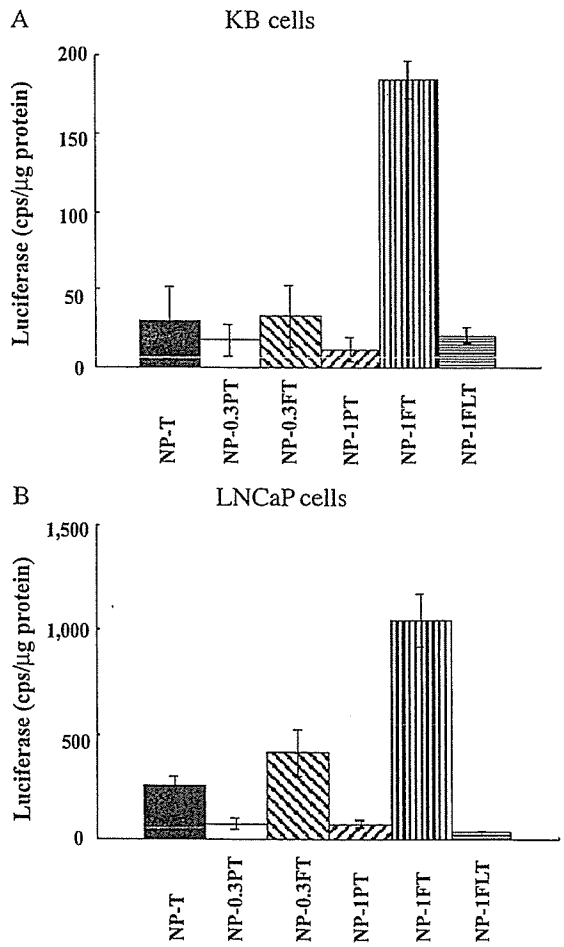

Fig. 4. Transfection into KB cells (A) and LNCaP cells (B) with FR-targeted nanoplex. Transfection particles were prepared by mixing the pCMV-Luc DNA with NPs. The cells were incubated for 24 h with transfection particles present at 2 μg DNA/ml in media with 10% serum. The cells were analyzed for luciferase activity. Each column represents the mean ± S.D. ($n=3$).

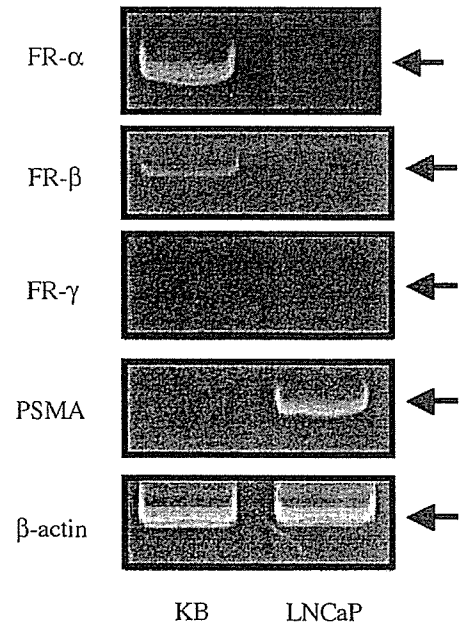

Fig. 5. FRs (FR-α, -β, -γ) and PSMA mRNA expression in KB and LNCaP cells by RT-PCR.

3.8. Expression of FRs and PSMA mRNA

Finally, to examine the mechanism of cellular uptake of folate-linked NPs, we investigated the expression of FRs in KB and LNCaP cells by RT-PCR method (Fig. 5). KB cells expressed strongly FR-α mRNA and weakly FR-β mRNA, but LNCaP cells did not. FR-γ did not express in both the cells. This suggested that FR-α and -β mediated the cellular uptake of folate-linked NPs in KB cells, but not LNCaP cells.

Therefore, it is suggested that the uptake in LNCaP cells was mediated by PSMA, and so we examined whether PSMA mRNA was expressed in LNCaP cells. PSMA mRNA was expressed strongly in LNCaP cells, but not in KB cells (Fig. 5).

4. Discussion

Although many cationic liposomes showed high gene transfer activity in vitro, their in vivo application remains limited due to their instability in serum [27]. The physical stability of the carrier and its complex

with DNA has been regarded as one of the most important factors [28]. When larger particles were administered systemically, they predominantly accumulated in the liver. This can be explained by its large mean size resulting in strong recognition of particles by the mononuclear phagocytes in the liver (Kupffer cells) [29]. A second mechanism involving the adsorption of lipoproteins on the particles cannot be ruled out. Due to the large positive ζ-potential associated with the nanoparticles, negatively charged lipoprotein present in serum would easily adsorb on its surface and accelerate the clearance from the circulation.

In preliminary experiments, we could prepare the injectable sized nanoplex using cationic NP composed of DC-Chol, f-PEG_{2000}-DSPE and PEG_{2000}-DSPE. Addition of PEG-lipid in NPs provided a stronger steric stabilization activity in the particles so that large aggregates of nanoplexes were no longer formed even in serum. However, these nanoplexes showed low transfection activity in LNCaP and KB cells (data not shown).

Recently, nonionic surfactants such as Tween 80 were used as additional additives in cationic liposomes or emulsions, presumably to enhance its physical stability [30,31]. Tween 80 may have a similar fusogenic property to DOPE and elicit its effect by stabilizing the liposomes. Therefore, addition of PEG-lipid and Tween 80 in NPs may have provided a stronger steric stabilization and fusogenic activities for the particles.

We developed cationic NPs composed of DC-Chol, Tween 80 and f-PEG-DSPE, which were given in the injectable size of about 215–300 nm (Table 2). f-PEG-DSPE and Tween 80 as a surfactant may have contributed to reduce the particle size and stabilize the nanoplex. It was reported that lipoplex is physically unstable and undergoes a change in overall structure when net charge of lipoplex approaches neutralization [3,4]. Unlike liposomes, when the ζ-potential of the nanoplexes approaches neutralization, the change in size of the nanoplexes may be minimal. Even in the presence of serum, the nanoplex did not aggregate and maintained its size (about 350 nm in NF-1FLT and about 500 nm in NP-1FT), suggesting that addition of 1 mol% PEG-DSPE and 5 mol% Tween 80 provides a stronger steric stabilization activity for the particles. This may be due to the ability of 1 mol% PEG and 5 mol% Tween 80 to shield almost completely the particle's residual positive charge.

The FR-specific delivery with DiI-labeled nanoplex of NP-1FT in KB cells was compared in the absence or presence of 1 mM folic acid in the medium. Cellular association of the nanoplex of NP-1FT with the cells was enhanced by the folate ligand (Fig. 2A) and reduced in the presence of free folic acid (Figs. 2B and 3A–D). This suggested that an association by interaction between the folate moiety of NP-1FT and FR of KB cells played a major route of transfection of nanoplex of NP-1FT.

FITC-labeled plasmid was detected strongly on the cell surface and weakly in cytoplasm (Fig. 3E and F). The colocalization of DiI and FITC signals was also detected on the cell surface, suggesting that the plasmid still bound to NP-1FT and stayed at the cell surface. Therefore, the nanoplex of NP-1FT bound to FR and then FR-mediated endocytosis may not have occurred rapidly. In addition, small amounts of PEG-lipid might prevent membrane fusion and cell internalization.

Tissue-targeted gene expression is an important issue for improvement of safety in gene therapy. Preferential expression of a gene in tumor cells contributes to the safety and the efficacy of gene therapy. The transfection efficiency of the luciferase gene was enhanced by folate-linked NPs. The highest luciferase activity in KB cells was observed in NP-1FT, and in LNCaP cells observed in NP-0.3FT and-1FT (Fig. 4), whereas low transfection activity was observed in all nonlinked NPs in both cells. NP-1FT showed slightly low transfection efficiency compared with that by Tfx20. This suggests the usefulness of NP-1FT as selective transfection reagents for the cells expressing folate binding protein. In the molecular weight of PEG, f-PEG_{2000}-DSPE will be suitable for high transfection with selectivity since f-PEG_{5000}-DSPE may reduce the cell association through steric hindrance. However, it is not clear why the different patterns of transfection activity in NP-0.3FT between the two kinds of cell lines were observed. The distribution density of folate binding protein on the cell surface in LNCaP cells might be higher than that in KB cells.

Finally, we investigated the expression of FRs in KB and LNCaP cells. There are three folate receptor isoforms, α, β and γ, with distinctive patterns of tissue distribution. FR-α is predominantly expressed

in most normal and malignant epithelial tissues [13,14], FR-β in some nonepithelial malignancies [16, 17] and FR-γ in hematopoietic cells [18,19]. FR-α and FR-β mRNA were expressed in KB cells (Fig. 5). The uptake of NPs in KB cells may be mediated via FR-α and-β.

PSMA is homologous to the transferrin receptor with an overexpression pattern restricted to prostate cancer cells and malignant human prostate tissue and is known to have the ability to remove the glutamate residues from folate-poly-γ-glutamate [23]. It was reported that human prostate contains folate-binding proteins [21], and that folic acid binds to the membrane fraction that cross-reacts with anti-PSMA antibody [23]. It is suggested that uptake of folate-linked NPs in LNCaP cells might be mediated by PSMA, and therefore we examined the expression of PSMA mRNA. In LNCaP cells, PSMA mRNA was abundantly expressed, but FR mRNAs were not (Fig. 5). This suggested that the folate-linked NPs bound to PSMA and then were taken up by LNCaP cells. This study is the first to report that folate-linked NPs can selectively deliver DNA to prostate cancer and then enhance the gene expression.

5. Conclusions

We have shown that NPs based on the DC-Chol, f-PEG_{2000}-DSPE and Tween 80 could form injectable nanoplexes with high transfection of the luciferase gene in human oral cancer and prostate cancer cells. Such folate-linked nanoparticles are potentially useful as prostate tumor-specific vectors for gene therapy. Further studies on in vivo gene delivery are now underway to evaluate the efficacy and safety of the present system.

Acknowledgements

We thank Mr. Tomonori Shiokawa and Mr. Masayoshi Fukushima for assistance in the experimental work. We also thank Dr. Kazuhiro Kubo (NOF, Tokyo, Japan) for supplying PEG-DSPE.

This project was supported in part by a grant from the Promotion and Mutual Aid Corporation for Private Schools of Japan and by a Grant-in-Aid for Scientific Research from the Ministry of Education, Culture, Sports, Science, and Technology of Japan.

References

[1] C.R. Dass, M.A. Burton, Lipoplexes and tumours. A review, J. Pharm. Pharmacol. 51 (1999) 755–770.
[2] D.A. Treco, R.F. Selden, Non-viral gene therapy, Mol. Med. Today 1 (1995) 314–321.
[3] B. Sternberg, F.L. Sorgi, L. Huang, New structures in complex formation between DNA and cationic liposomes visualized by freeze-fracture electron microscopy, FEBS Lett. 356 (1994) 361–366.
[4] E. Lai, J.H. van Zanten, Real time monitoring of lipoplex molar mass, size and density, J. Control. Release 82 (2002) 149–158.
[5] N.K. Egilmez, Y. Iwanuma, R.B. Bankert, Evaluation and optimization of different cationic liposome formulations for in vivo gene transfer, Biochem. Biophys. Res. Commun. 221 (1996) 169–173.
[6] M. Nishikawa, L. Huang, Nonviral vectors in the new millennium: delivery barriers in gene transfer, Hum. Gene Ther. 12 (2001) 861–870.
[7] J.A. Reddy, D. Dean, M.D. Kennedy, P.S. Low, Optimization of folate-conjugated liposomal vectors for folate receptor-mediated gene therapy, J. Pharm. Sci. 88 (1999) 1112–1118.
[8] M.A. Gosselin, R.J. Lee, Folate receptor-targeted liposomes as vectors for therapeutic agents, Biotechnol. Annu. Rev. 8 (2002) 103–131.
[9] J.A. Reddy, C. Abburi, H. Hofland, S.J. Howard, I. Vlahov, P. Wils, C.P. Leamon, Folate-targeted, cationic liposome-mediated gene transfer into disseminated peritoneal tumors, Gene Ther. 9 (2002) 1542–1550.
[10] H.E. Hofland, C. Masson, S. Iginla, I. Osetinsky, J.A. Reddy, C.P. Leamon, D. Scherman, M. Bessodes, P. Wils, Folate-targeted gene transfer in vivo, Mol. Ther. 5 (2002) 739–744.
[11] J. Sudimack, R.J. Lee, Targeted drug delivery via the folate receptor, Adv. Drug Deliv. Rev. 41 (2000) 147–162.
[12] S. Ni, S.M. Stephenson, R.J. Lee, Folate receptor targeted delivery of liposomal daunorubicin into tumor cells, Anticancer Res. 22 (2002) 2131–2135.
[13] P.C. Elwood, Molecular cloning and characterization of the human folate-binding protein cDNA from placenta and malignant tissue culture (KB) cells, J. Biol. Chem. 264 (1989) 14893–14901.
[14] M. Wu, W. Gunning, M. Ratnam, Expression of folate receptor type alpha in relation to cell type, malignancy, and differentiation in ovary, uterus, and cervix, Cancer Epidemiol. Biomark. Prev. 8 (1999) 775–782.
[15] F. Shen, J.F. Ross, X. Wang, M. Ratnam, Identification of a novel folate receptor, a truncated receptor, and receptor type beta in hematopoietic cells: cDNA cloning, expression, immunoreactivity, and tissue specificity, Biochemistry 33 (1994) 1209–1215.
[16] M. Ratnam, H. Marquardt, J.L. Duhring, J.H. Freisheim, Ho-

mologous membrane folate binding proteins in human placenta: cloning and sequence of a cDNA, Biochemistry 28 (1989) 8249–8254.
[17] J.F. Ross, H. Wang, F.G. Behm, P. Mathew, M. Wu, R. Booth, M. Ratnam, Folate receptor type beta is a neutrophilic lineage marker and is differentially expressed in myeloid leukemia, Cancer 85 (1999) 348–357.
[18] H. Wang, J.F. Ross, M. Ratnam, Structure and regulation of a polymorphic gene encoding folate receptor type gamma/gamma', Nucleic Acids Res. 26 (1998) 2132–2142.
[19] X. Wang, G. Jansen, J. Fan, W.J. Kohler, J.F. Ross, J. Schornagel, M. Ratnam, Variant GPI structure in relation to membrane-associated functions of a murine folate receptor, Biochemistry 35 (1996) 16305–16312.
[20] X. Gao, A.T. Porter, D.J. Grignon, J.E. Pontes, K.V. Honn, Diagnostic and prognostic markers for human prostate cancer, Prostate 31 (1997) 264–281.
[21] J. Holm, S.I. Hansen, M. Hoier-Madsen, High-affinity folate binding in human prostate, Biosci. Rep. 13 (1993) 99–105.
[22] D.A. Silver, I. Pellicer, W.R. Fair, W.D. Heston, C. Cordon-Cardo, Prostate-specific membrane antigen expression in normal and malignant human tissues, Clin. Cancer Res. 3 (1997) 81–85.
[23] J.T. Pinto, B.P. Suffoletto, T.M. Berzin, C.H. Qiao, S. Lin, W.P. Tong, F. May, B. Mukherjee, W.D. Heston, Prostate-specific membrane antigen: a novel folate hydrolase in human prostatic carcinoma cells, Clin. Cancer Res. 2 (1996) 1445–1451.
[24] A. Gabizon, A.T. Horowitz, D. Goren, D. Tzemach, F. Mandelbaum-Shavit, M.M. Qazen, S. Zalipsky, Targeting folate receptor with folate linked to extremities of poly(ethylene glycol)-grafted liposomes: in vitro studies, Bioconjug. Chem. 10 (1999) 289–298.
[25] J. Zabner, Cationic lipids used in gene transfer, Adv. Drug Deliv. Rev. 27 (1997) 17–28.
[26] V. Escriou, C. Ciolina, F. Lacroix, G. Byk, D. Scherman, P. Wils, Cationic lipid-mediated gene transfer: effect of serum on cellular uptake and intracellular fate of lipopolyamine/DNA complexes, Biochim. Biophys. Acta 1368 (1998) 276–288.
[27] D.L. Reimer, S. Kong, M. Monck, J. Wyles, P. Tam, E.K. Wasan, M.B. Bally, Liposomal lipid and plasmid DNA delivery to B16/BL6 tumors after intraperitoneal administration of cationic liposome DNA aggregates, J. Pharmacol. Exp. Ther. 289 (1999) 807–815.
[28] O. Zelphati, C. Nguyen, M. Ferrari, J. Felgner, Y. Tsai, P.L. Felgner, Stable and monodisperse lipoplex formulations for gene delivery, Gene Ther. 5 (1998) 1272–1282.
[29] T. Sakaeda, K. Hirano, Effect of composition on biological fate of oil particles after intravenous injection of O/W lipid emulsions, J. Drug Target. 6 (1998) 273–284.
[30] F. Liu, J. Yang, L. Huang, D. Liu, Effect of non-ionic surfactants on the formation of DNA/emulsion complexes and emulsion-mediated gene transfer, Pharm. Res. 13 (1996) 1642–1646.
[31] T.W. Kim, H. Chung, I.C. Kwon, H.C. Sung, S.Y. Jeong, Optimization of lipid composition in cationic emulsion as in vitro and in vivo transfection agents, Pharm. Res. 18 (2001) 54–60.

5

機能性脂質マイクロエマルションとDDS

米谷 芳枝*
Maitani Yoshie

Summary

機能性脂質マイクロエマルションとして，注射用血中滞留性マイクロエマルション，葉酸修飾マイクロエマルション，トリプシン修飾遺伝子ベクター，鼻腔投与用キトサン被覆マイクロエマルションを調製し，癌化学療法，癌遺伝子治療，粘膜ワクチンに応用した。血中滞留性マイクロエマルションは，マイクロエマルションをポリエチレングリコール（PEG）脂質で修飾して調製し，アクラルビシン，ビンクリスチン，パクリタキセルを封入した。葉酸修飾マイクロエマルションは，血中滞留性マイクロエマルションのPEG脂質の先端の一部を葉酸で修飾し，癌組織に高発現している葉酸受容体に，抗癌薬をターゲティングする，癌ターゲティング治療を目指した。トリプシン修飾マイクロエマルション遺伝子ベクターでは，癌細胞周辺の組織を破壊して，癌細胞にまで遺伝子を運べるように，エマルションの表面をトリプシンで修飾した。キトサン被覆マイクロエマルションワクチン製剤は，正電荷で鼻粘膜に付着し，抗原提示細胞に取り込まれ，IgA（イムノグロブリンA）を産生した。

1．はじめに

微粒子製剤は，薬物を標的部位に集積させて，副作用を軽減し，薬効を高めることができるので，DDS（drug delivery system；薬物送達システム）において注目されている。薬物の微粒子担体には，マイクロスフェア，マイクロカプセル，リポソーム，エマルション，高分子ミセルなどがある。エマルションにおいて，界面活性剤としてリン脂質を使ったものを，特に，脂肪乳剤という。私達のマイクロエマルションの特徴は，ナノサイズのエマルションを簡単な調製法で，表面修飾して機能性マイクロエマルションにしている点である。機能性脂質マイクロエマルションには，PEG（polythylene glycol）脂質で修飾した血中滞留性エマルションや，癌ターゲティング用葉酸修飾マイクロエマルションやトリプシン修飾遺伝子ベクターがある。（図1）。ここでは，機能性マイクロエマルション製剤による，癌化学療法，遺伝子治療，免疫治療への応用について紹介する。

2．マイクロエマルション

一般には，エマルションは，水に油と乳化剤を加えて機械的に乳化して調製される。その粒子サイズは，約0.2～10 μm のものが多い。マイクロエマルションの定義は，元来は，瞬時に調製され，

*星薬科大学医薬品化学研究所創剤構築研究室・教授

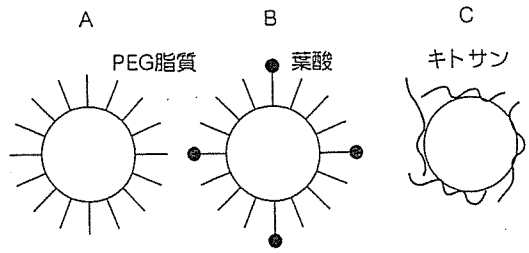

図1 血中滞留性マイクロエマルション（A），葉酸修飾マイクロエマルション（B），キトサン被覆マイクロエマルション（C）
PEG脂質で表面修飾したマイクロエマルション（A），PEG脂質の先端の一部を葉酸で修飾した癌ターゲティング用マイクロエマルション（B），正電荷マイクロエマルション（C）．
PEG：polyethylene glycol

透明で安定なエマルションという意味で，小さなサイズの油滴という意味ではないが，現在，両方の意味で広義に用いられている。

エマルションの利点は，脂肪乳剤に代表されるように，製剤としての安全性や安定性が高いこと，また，多くの薬物で見られる，難水溶性の薬物を溶解できること，などである。欠点は，親水性薬物は封入できないこと，などである。これまでに，点滴注射用脂肪乳剤や経口投与製剤が市販されている。経口投与製剤では，シクロスポリンMEPC(micro-emulsion pre-concentrate，前濃縮物製剤)(ネオーラル®)が商品化されている[1]。これは，自己乳化システム（self-emulsifying drug delivery systems，SEDDS）で，薬物と油と界面活性剤溶液を，ゼラチンカプセルに詰めたもので，飲んだ水でエネルギーを加えることなく，腸管内で瞬時にマイクロエマルションを形成する。

私達のマイクロエマルションも同じように，脂質をエタノールに溶解し，濃縮後，水を添加すると瞬時に形成される。(図2)。この方法で，ナノサイズの微粒子を，超音波などのような外部からのエネルギーや，有害な有機溶媒を用いず，短時間に調製できる[2]。

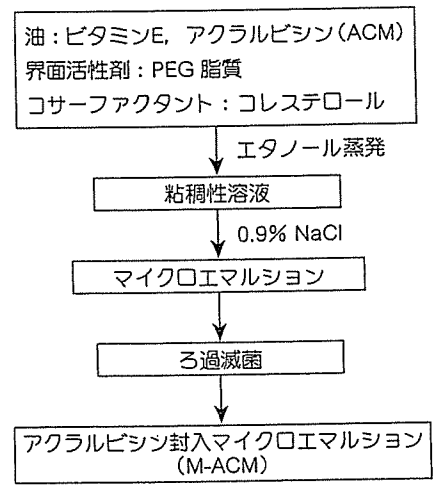

図2 注射用マイクロエマルション調製法
ビタミンEの油にACMを溶かし，これとPEG脂質，コレステロールをエタノールに溶解後，エタノールを蒸発させ，水を加えると，直ちにマイクロエマルションが形成される。

3．注射用抗癌剤封入血中滞留性マイクロエマルション製剤

一般に，微粒子は，静脈内投与すると，血液成分との相互作用ののち，単核食細胞系に認識され，体循環血から除去される。そこで，血中滞留性エマルションでは，血液成分を吸着しにくくするために，PEGで修飾した。腫瘍部位では，血管壁がうすく，薬液が漏れやすくなっているので，血中滞留性リポソームは，抗癌剤の腫瘍部位への集積（受動的ターゲティング）が可能となる。既に，ドキソルビシン血中滞留性リポソーム製剤(Doxil®)が，欧米では発売されている。しかし，血中滞留性エマルションは，研究報告もまだ極めて少ない。血中滞留性エマルションでは，リポソームに封入しにくい疎水性薬物の，腫瘍部位への受動的ターゲティングが可能となる。

塩酸アクラルビシン(アクラシノン，ACM)，硫酸ビンクリスチン(オンコビン，VCR)，パクリタキセル（タキソール® ）は，疎水性薬物で，リポソームに封入しにくく，水溶液中で不安定である。そこで，界面活性剤とコサーファクタントとして，コレステロールとPEG脂質からなる，アク

ラルビシン封入血中滞留性エマルション（M-ACM）[3]，ビンクリスチン封入血中滞留性マイクロエマルション（M-VCR）[4]，パクリタキセル（Paclitaxel）封入血中滞留性マイクロエマルション（M-Paclitaxel）[5]を開発した。PEG脂質は，血中滞留性の機能だけでなく，両親媒性で良い乳化剤となるので，マイクロエマルションを調製しやすい[6]。M-ACMやM-VCRの平均粒子サイズは140nm以下で，薬物封入率は95%以上であった。また，遮光下7℃で1年間の保存では，製剤として安定であった。

M-ACMでは，マウスにおいて，ACMの血中滞留性が高くなり，固形癌に対する抗腫瘍効果も，フリーのACMに比べて投与量に応じて高くなった。M-VCRもマウスにおいて血中滞留性を示し，VCRが腫瘍に蓄積して，固形癌に対する抗腫瘍効果もフリーの薬物に比べて高くなった[4]。（図3，表1）。

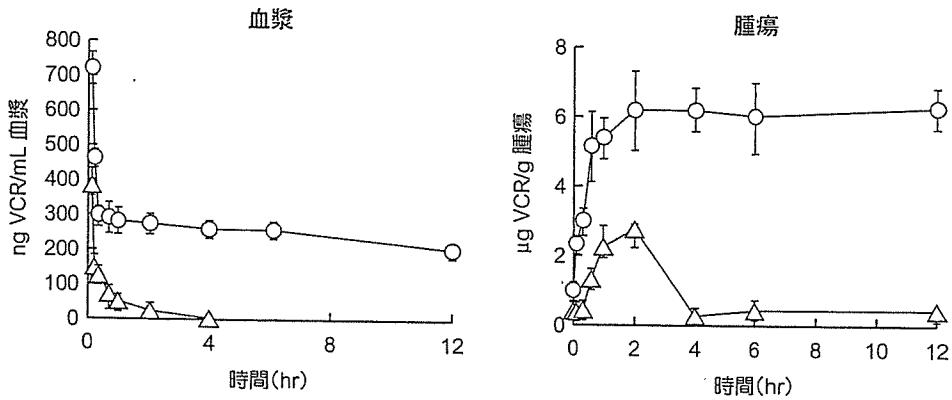

図3　ビンクリスチン封入マイクロエマルション（M-VCR）の体内動態
○：M-VCR，△：フリーVCR（ビンクリスチン生理食塩水〔0.1mg/mL〕）
ビンクリスチン封入マイクロエマルションを2 mg/kgマウスでM5076固形癌のマウスに静脈内投与したときの血中濃度と腫瘍内薬物濃度の時間変化．
マイクロエマルションでは，薬物は注射12時間後でも血中に検出され，固形癌に集積した．
（文献4より）

表1　ビンクリスチン封入マイクロエマルション（M-VCR）の抗腫瘍効果
VCR封入マイクロエマルションの固形癌に対する抗腫瘍効果は，フリーの薬物に比べて高くなった．

製剤	投与量 (mg VCR/kg)	腫瘍重量 (g ± SD)	腫瘍重量減少率 (%)	
生理食塩液	コントロール	1.2 ± 0.2	---	
M（薬物不含）	コントロール	1.2 ± 0.3	0	
フリーVCR	1.25	0.7 ± 0.2	42	*
M-VCR	1.25	0.4 ± 0.2	67	*

腫瘍を移植後，5日目に5日ごとに4回繰り返し静脈内投与．
＊：$p < 0.01$
M：薬物封入マイクロエマルション
フリーVCR：ビンクリスチン生理食塩水（0.1mg/mL）
M-VCR：ビンクリスチン封入マイクロエマルション
（文献4より）

M-Paclitaxelでは，難溶性である薬物を，界面活性剤とコサーファクタントとして，PEG脂質やコレステロール，Tween80と大豆油を用いて，薬物封入率の高いマイクロエマルション製剤とした。M-Paclitaxelの薬物分布の模式図を，図4に示す。薬物は，油滴の内部と表面に，分布していると考えられる。人工ニュラルネットワークを用いて，各成分の製剤に対する寄与を解析すると，PEG脂質は薬物封入率と粒子サイズに，Tween80は製剤の安定性に，それぞれ関与していることが明らかになった[5]。

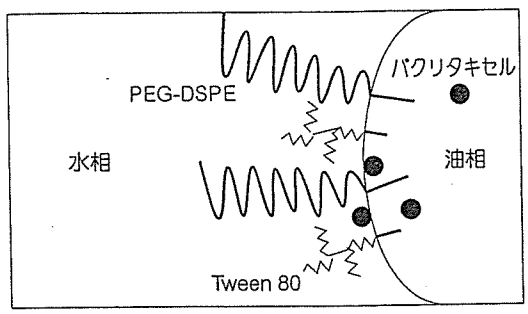

図4　パクリタキセル封入マイクロエマルション（o/w）の薬物分布の模式図

マイクロエマルションの平均粒子径は262nmで，薬物を96.7%含有した．薬物は，油滴の内部と表面に分布し，PEG脂質が薬物封入率と粒子サイズに，Tween80が製剤の安定性にそれぞれ関与している．

o/w：oil in water

PEG-DSPE：polyethylene glycol-distearoylphosphatidyl ethanolamine

4．注射用アクラルビシン封入葉酸修飾マイクロエマルション製剤

葉酸受容体は，卵巣，乳房，結腸，肺の上皮癌などにおいて，過剰発現していることが知られているので，葉酸をリガンドとした担体は，癌細胞にターゲティングが可能となる。従って，アクラルビシン封入葉酸修飾マイクロエマルション（FM-ACM）は，PEG修飾によって血中滞留したM-ACMに，さらに一部のPEG鎖の先端を，葉酸によって修飾したものである。FM-ACMは，葉酸脂質あるいは，葉酸-PEG脂質（PEG分子量2,000，5,000）（図5），PEG脂質（分子量2,000），コレステロール，ビタミンEを含有する。

葉酸修飾による細胞内への，ターゲティング能を評価するため，蛍光ラベル物質である1,1'-

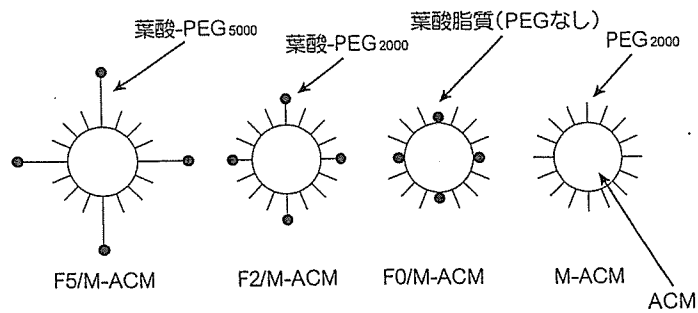

図5　アクラルビシン（ACM）封入葉酸修飾マイクロエマルション

マイクロエマルションは，葉酸-PEG脂質：PEG脂質：コレステロール：ビタミンE：ACM＝0.24：6.7：48.3：43.3：1.5(mol%)で，平均粒子径は約120nm，ACM封入率約80%である．

PEG：polyethylene glycol. PEGの後ろにある数値は，分子量．

F5/M-ACM：葉酸-PEG脂質（5,000）で修飾したM-ACM

F2/M-ACM：葉酸-PEG脂質（2,000）で修飾したM-ACM

F0/M-ACM：葉酸脂質で修飾したM-ACM

M-ACM：封入マイクロエマルション（PEG脂質2,000からなるエマルション）

ACM：アクラルビシン　（文献7より）

Dioctadecyl-3,3,3',3'-tetramethylindocarbocyanine perchlorate (DiI) でラベルした，葉酸修飾マイクロエマルションの，ヒト咽頭上皮癌細胞（KB 細胞）への取り込み量を測定した結果，葉酸修飾によって，取り込みは高くなった。また，フリーの葉酸により，取り込みが阻害されることから，競合阻害が起きていると考えられ，細胞内への取り込みは，葉酸受容体を介していることが確認された。また，葉酸修飾 PEG 脂質の PEG 鎖の長さによる，葉酸受容体の認識能への影響を，*in vitro* 抗癌作用から調べた結果，PEG 脂質の PEG 鎖が，分子量 5,000（F5/M-ACM）のとき，2,000（F2/M-ACM）のときよりも，細胞内への ACM の取り込みが高くなった。（図 6）。担癌マウスにおける抗

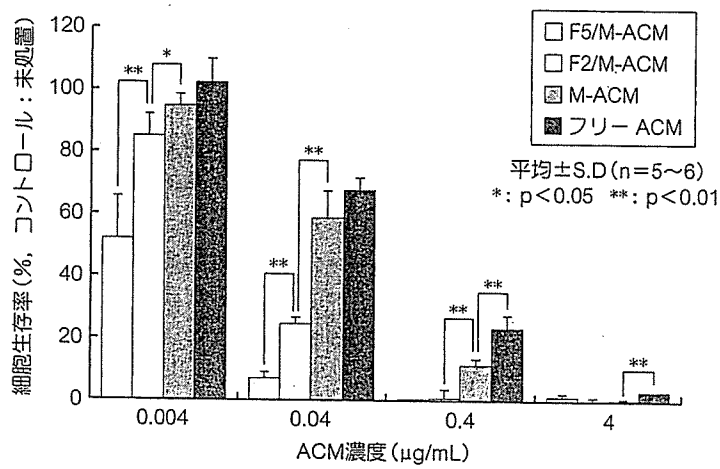

図 6　アクラルビシン封入葉酸修飾マイクロエマルションの *in vitro* 抗腫瘍効果
PEG 鎖 5,000 に葉酸修飾したマイクロエマルション F5/M-ACM は，細胞生存率を低下し，高い抗腫瘍効果を示した．この効果はフローサイトメトリーによる細胞への取り込み量と相関するものであった．
PEG：polyethylene glycol
F5/M-ACM：葉酸-PEG 脂質（5,000）で修飾した M-ACM
F2/M-ACM：葉酸-PEG 脂質（2,000）で修飾した M-ACM
M-ACM：封入マイクロエマルション（PEG 脂質 2,000 からなるエマルション）
フリー ACM：ACM 生理食塩水
（文献 7 より）

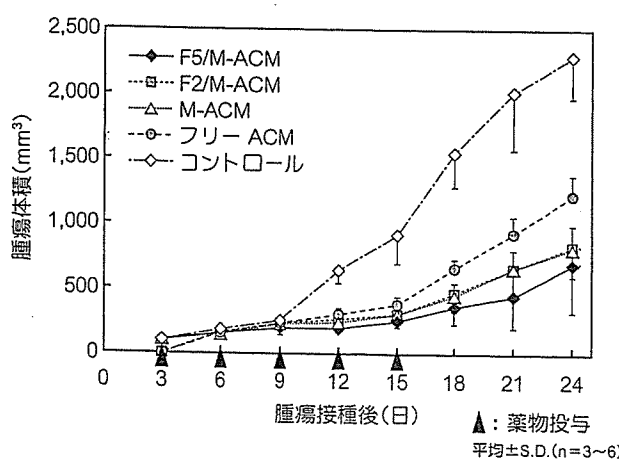

図 7　アクラルビシン封入葉酸修飾マイクロエマルション静脈内投与による抗腫瘍効果
F5/M-ACM は最も高い抗腫瘍効果を示した．葉酸修飾マイクロエマルションは *in vivo* においても有用であることが確認された．
F5/M-ACM：葉酸-PEG 脂質（5,000）で修飾した M-ACM
F2/M-ACM：葉酸-PEG 脂質（2,000）で修飾した M-ACM
M-ACM：封入マイクロエマルション（PEG 脂質 2,000 からなるエマルション）
フリー ACM：ACM 生理食塩水
control：生理食塩水　（文献 7 より）

腫瘍効果より，マイクロエマルション製剤を葉酸で修飾することにより，ACMの高い抗癌作用が得られた。特に，葉酸修飾PEG鎖が分子量5,000のとき，ターゲティング能が高くなることが明らかになった[7]。(図7)。

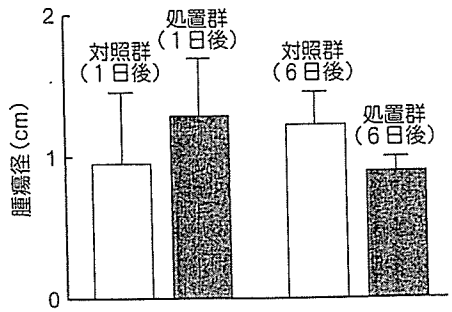

図8 ミドカインプロモータ自殺遺伝子とトリプシン修飾血中滞留性マイクロエマルションベクターによる自殺遺伝子治療における抗腫瘍効果

ヒト膵臓固形癌のサイズが約1cmになったとき，ベクター/遺伝子の荷電比＝4/1で自殺遺伝子とガンシクロビルを10μg/腫瘍で2日間ごとに2回腫瘍内注射した．(平均±SD，n＝3)

遺伝子導入の結果，腫瘍の縮小が観察された．

(文献8より)

5．トリプシン修飾マイクロエマルション遺伝子ベクター

外来遺伝子の導入による癌治療の1つに，プロドラッグ療法の自殺遺伝子治療がある。これは，腫瘍部位に導入した，単純ヘルペスウイルスチミジンキナーゼ(HSV-tk)がチミジンキナーゼ(tk)を発現させ，この酵素によって，プロドラッグが活性代謝物になって，癌細胞を死滅させるものである。腫瘍細胞特異的に，治療遺伝子を発現させて，腫瘍の治療を行うために，腫瘍細胞特異的に，遺伝子を運搬する微粒子と，腫瘍細胞内で，導入遺伝子を，特異的に発現させるプロモータを選択した。ミドカインは，消化器系癌や神経芽腫など，色々な癌の進行癌に，高頻度に発現している。従って，癌ターゲティングのために，ミドカインプロモータのtk遺伝子を用いた。微粒子担体としては，トリプシン修飾して，癌細胞周辺の組織を破壊して，癌細胞にまで遺伝子を運べるように，トリプシン修飾血中滞留性マイクロエマルションベクターをデザインした。これは，油相としてビタミンE，また界面活性剤とコサーファクタントとして，DC-コレステロール，コレステ

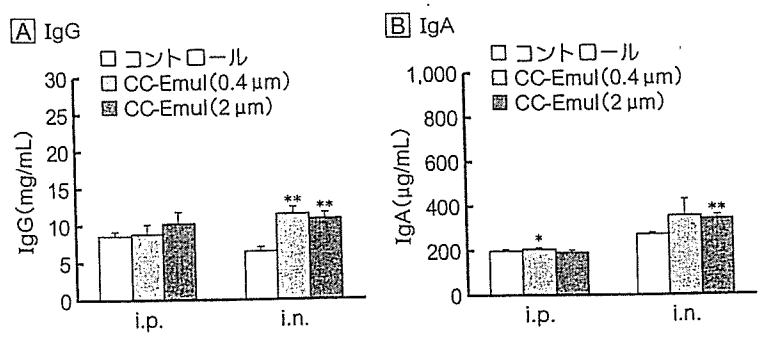

図9 オブアルブミンとコレラトキシンを吸着させた粒子径約0.4μmと2μmのキトサン被覆エマルション(CC-Emul)をラット腹腔内と鼻腔投与したときのIgG(A)とIgA(B)

投与は0，14，28日目にして，35日目に採血した．平均値±S.D(n＝3～5)．＊：p＜0.05，＊＊：p＜0.01コントロールと比較．コントロールはオブアルブミン(5mg/kg)とコレラトキシン(2.5mg/kg)のみ．粒子径約2mmのCC-Emulの鼻腔内投与は，腹腔内投与より高く，コントロールに対して有意に高いIgGとIgAを産生した．

(文献9より)

ロールとPEG脂質とオレイン酸からなる。マイクロエマルションを調製後，オレイン酸の先端に，トリプシンを結合させた。遺伝子導入の結果，ヒト膵臓固形癌ヌードマウスにおいて，腫瘍の縮小が観察された[8]。(図8)。

6．経鼻吸収用キトサン被覆マイクロエマルションワクチン製剤

ワクチン製剤の多くは，皮下または筋肉内投与によって，行われている。これらの投与方法は侵襲的であるので，粘膜投与によるワクチン製剤の送達は，粘膜免疫と呼ばれ，近年盛んに研究が行われている。鼻腔に投与された微粒子は，抗原提示細胞(APC)によって，抗原提示が起こると考えられている。従って，APCに取り込まれやすい微粒子として，正電荷で鼻粘膜に付着し，鼻粘膜附属リンパ組織(NALT)のM細胞への取り込みを促進する，キトサン被覆マイクロエマルションワクチン製剤を検討した。0.4～3 μmのキトサン被覆マイクロエマルションは，オブアルブミンの付着率が高く，なおかつ正電荷を有するワクチン製剤である。また，鼻粘膜投与において，腹腔内投与とほぼ同等の高い，IgG抗体とIgA抗体の産生を示した。また，NALTとAPCの取り込みに対する，エマルション製剤の粒子径の影響は，ナノパーティクルほど明確ではなかった[9]。(図9)。

7．おわりに

癌細胞に，特異的な発現をした抗体や受容体と親和性がある，リガンドを用いた精密なターゲティングを可能とするには，まず，体内動態を制御できる，機能性微粒子担体の開発が必須である。機能性脂質マイクロエマルションは，その1つとして有望である。

参考文献

1) 高原史郎：腎移植患者におけるシクロスポリンMEPCの薬物動態試験－現行製剤を対照とした交差比較二重盲検試験－．今日の移植 12：5-24, 1999.
2) Maitani Y, et al：Modified ethanol injection method for liposomes containing β-sitosterol β-D-glucoside. J Liposome Res 11 (1)：115-125, 2001.
3) Wang J, et al：Antitumor effects and pharmacokinetics of aclacinomycin A carried by injectable emulsions composed of vitamin E, cholesterol and PEG-lipid. J Pharm Sci 91 (4)：1128-1134, 2002.
4) Wang J, et al：Pharmacokinetics and antitumor effects of vincristine carried by microemulsions composed of and PEG-lipid, oleic acid, vitamin E and cholesterol. Int J Pharm 251 (1-2)：13-21, 2003.
5) Fan T, et al：Formulation optimization of paclitaxel carried by pegylated emulsions based on artificial neural network. Pharm Res 21 (9)：1694-1699, 2004.
6) Liu F, et al：Long-circurating emulsions (oil-in-water) as carriers for lipophilic drugs. Pharm Res 12：1060-1064, 1995.
7) Shiokawa T, et al：Effect of the PEG-linker Chain Length of Folate-linked Microemulsions Loading Aclacinomycin A on Targeting Ability and Antitumor Effect *in vitro* and *in vivo*. 投稿中
8) Wang J, et al：Preparation and antitumor effects of trypsin-modified PEGlated microemulsions as carrier of suicide gene controlled by tumor-targeting promoter. 第122年会日本薬学会要旨集 4：78, 2002.
9) Nagamoto T, et al：Novel chitosan particles and chitosan-coated emulsions inducing immune response via intranasal vaccine delivery. Pharm Res 21：671-674, 2004.

Formulation Optimization of Paclitaxel Carried by PEGylated Emulsions Based on Artificial Neural Network

Tianyuan Fan,[1] Kozo Takayama,[2] Yoshiyuki Hattori,[3] and Yoshie Maitani[3,4]

Received March 7, 2004; accepted May 16, 2004

Purpose. To develop paclitaxel carried by injectable PEGylated emulsions, an artificial neural network (ANN) was used to optimize the formulation—which has a small particle size, high entrapment efficiency, and good stability—and to investigate the role of each ingredient in the emulsion.

Methods. Paclitaxel emulsions were prepared by a modified ethanol injection method. A computer optimization technique based on a spherical experimental design for three-level, three factors [soybean oil (X1), PEG-DSPE (X2) and polysorbate 80 (X3)] were used to optimize the formulation. The entrapment efficiency of paclitaxel (Y1) was quantified by HPLC; the particle size of the emulsions (Y2) was measured by dynamic laser light scattering and the stability of paclitaxel emulsions was monitored by the changes in drug concentration (Y3) and particle size (Y4) after storage at 4°C.

Results. The entrapment efficiency, particle size and stability of paclitaxel emulsions were influenced by PEG-DSPE, polysorbate 80, and soybean oil. Paclitaxel emulsions of small size (262 nm), high entrapment efficiency (96.7%), and good stability were obtained by the optimization.

Conclusions. A novel formulation for paclitaxel emulsions was optimized with ANN and prepared. The contribution indices of each component suggested that PEG-DSPE mainly contributes to the entrapment efficiency and particle size of paclitaxel emulsions, while polysorbate 80 contributes to stability.

KEY WORDS: artificial neural network; emulsions; optimization; paclitaxel; PEGylated..

INTRODUCTION

Paclitaxel is widely used as an effective anticancer agent for ovarian, colon, and breast cancer. The commercially available product, Taxol (paclitaxel), is currently a formulation of vehicle containing approximately a 1:1 vol/vol mixture of polyoxyethylated castor oil (Cremophor EL) and ethanol due to its extremely poor solubility in water (0.6 mM) and other pharmaceutical agents. Cremophor EL has been associated with hypersensitivity reactions, nephrotoxicity and neurotoxicity (1). Therefore, premedication with corticosteroids and antihistamine as well as long-term infusion of a 5–20-fold dilution of the product is required to reduce the side effects. However, there are a serious problems associated with dilution of the formulation such as compatibility and stability. The stability of diluted paclitaxel was estimated at 12–24 h since its use was recommended within 12 h of dilution in aqueous medium. Thus there is need for a new formulation of paclitaxel that is efficacious and less toxic than the commercial product.

Recently, many alternative formulations have been developed, such as emulsions (2–7), microspheres (8,9), liposomes (10,11), mixed micelles (12,13), cyclodextrins (14,15), and conjugates (16,17). Several compounds are often used in formulations of paclitaxel, such as polysorbate 80, PEG400, poloxamer, PEGylated lipid, and so forth. A common characteristic of the molecular structure of these compounds is the presence of a polyethyleneglycol group of different lengths and shapes. In fact, a polyethyleneglycol group also exists in the molecular structure of Cremophor EL.

The emulsion (o/w) used for the delivery of paclitaxel has attracted much attention (1). Triacetin provides a high level of solubility, 75 mg/ml, and has been used together with lecithin, pluronic F-68, polysorbate 80 and glycerol to produce a paclitaxel-containing emulsion (2). Wheelar *et al.* (3) manufactured a blend of emulsion and liposome with corn oil, EPC, cholesterol, PEG-lipid (polyethylene glycol derivative, mean molecular weight of PEG 2000) and paclitaxel. Lunberg (4) prepared a paclitaxel emulsion made of triolein, dipalmytoylphosphatidylcholine and polysorbate 80, with polyethylene glycol coated on the emulsion surface. Kan *et al.* (5) developed a paclitaxel emulsion with an oil blend of triacylglycerol, EPC and polysorbate 80 in a glycerol solution, while Simamora *et al.* (6) used polysorbate 80 and sorbitan monolaurate, and Constantinides *et al.* (7) used α-tocopherol, α-tocopherylpolyethyleneglycol-1000 succinate (TPGS), Poloxamer 407 and PEG 400. The optimization of these formulations was based on experience, not computer modeling. Also, the role of each ingredient in the formulation was not elucidated.

Recently we have reported injectable PEGylated emulsions composed of vitamin E, cholesterol and PEG-DSPE (polyethylene glycol derivative of distearoylphosphatidylethanolamine, mean molecular weight of PEG 2000) and an anticancer drug prepared by a modified ethanol injection method (18,19). Such PEGylated emulsions also might encapsulate paclitaxel. We tried to develop a Cremophor-free oil-in-water emulsion of paclitaxel using soybean oil as the internal phase, and polysorbate 80, PEG-DSPE and cholesterol as emulsifiers or co-emulsifiers.

Response surface techniques incorporating an artificial neural network (ANN) and the second-order polynomial regression equation (2PE) were used to achieve an optimal emulsion of paclitaxel with a small particle size, high entrapment efficiency and good stability. The application of ANN in the field of pharmaceutical development has gained interest in recent years (20–22). ANN is a learning system based on a computational technique that can simulate the neurologic processing ability of the human brain (23). Using a computor-program, ALCORA, it can also perform a classic opti-

[1] Department of Pharmaceutics, School of Pharmaceutical Sciences, Peking University, Beijing 100083, China.
[2] Department of Pharmaceutics, Hoshi University, Shinagawa-ku, Tokyo 142, Japan.
[3] Institute of Medicinal Chemistry, Hoshi University, Shinagawa-ku, Tokyo 142, Japan.
[4] To whom correspondence should be addressed. (e-mail: yoshie@hoshi.ac.jp)

ABBREVIATIONS: EPC, egg phosphatidylcholine; PEG-DSPE, polyethylene glycol derivative of distearoylphosphatidylethanolamine, mean molecular weight of PEG 2000; PEG 400, polyethylene glycol 400; ANN, artificial neural network; 2PE, the second-order polynomial regression equation.

0724-8741/04/0900-1692/0 © 2004 Springer Science+Business Media, Inc.

mization technique based on 2PE. The basic concepts of ALCORA and simultaneous optimization of several responses based on ANN have been described fully (24–27).

The aim of the study was to achieve, by applying an optimization, an optimal PEGylated emulsion containing paclitaxel which has a small size, high entrapment efficiency for paclitaxel and good stability, and to investigate the role of each ingredient in the emulsion using the response surface technique.

MATERIALS AND METHODS

Materials

Paclitaxel was kindly supplied by Bristol Pharmaceuticals K.K. (Tokyo, Japan). PEG-DSPE was purchased from NOF Co. Ltd (Tokyo, Japan). Soybean oil and glucose were obtained from Wako Pure Chemical Industries, Ltd (Tokyo, Japan). Cholesterol and polysorbate 80 were purchased from Tokyo Kasei Kogyo Co. Ltd. (Tokyo, Japan). PEG 400 was purchased from Kishida Chemical Co. Ltd. (Osaka, Japan). Chemicals for high-pressure liquid chromatography (HPLC) were of HPLC grade and all other chemicals were of analytical grade.

Preparation of Paclitaxel Emulsions

Paclitaxel emulsions were prepared by a modified ethanol injection method (18,19,28). Paclitaxel, soybean oil, PEG-DSPE, cholesterol, PEG 400 and polysorbate 80 were dissolved in 40 ml ethanol, then the ethanol was removed with a rotary evaporator till 1–2 ml was left. Next, a constant volume of 5% glucose solution was added to the ethanol solution. The emulsions formed instantly after further evaporation of the residual ethanol. The concentration of paclitaxel was adjusted to 0.6 mg/ml in the final emulsions containing the 5% glucose solution as external phase with drops of Milli Q water. Then the emulsions were filtrated through 0.45-μm Ekikrodisc filters (Gelman Japan, Tokyo, Japan) to homogenize the droplets of emulsion and stored at 4°C for further detection.

HPLC

The HPLC system was composed of an LC-10AS pump (Shimadzu Co., Ltd., Kyoto, Japan), a SIL-10A auto injector (Shimadzu Co., Ltd.), an SPD-10A UV detector (Shimadzu Co., Ltd.), and a C_{18} 4.6 × 150 mm reverse phase column (Shiseido, Tokyo, Japan; Capcell-park, 3 μm particle size). The mobile phase consisted of acetonitrile-0.1% phosphoric acid (wt/vol) in Milli Q water (55:45, vol/vol), at a flow rate of 1.0 ml/min. Chromatography was performed at ambient temperature (20 ± 2°C). The concentration of paclitaxel in each sample was determined with a constructed calibration curve. The internal standard was n-hexyl p-hydroxyl benzoic acid (Tokyo Kasei Kogyo Co., Tokyo, Japan). For UV detection, the wavelength was set to 227 nm (29).

Particle Size and Entrapment Efficiency

The particle size of paclitaxel emulsions was determined using a laser light scattering instrument (ELS800, Otsuka Electronics, Osaka, Japan) by the dynamic light scattering method.

The entrapment efficiency of paclitaxel emulsions was taken as the percentage of paclitaxel carried by the emulsions and was determined by two methods; Sephadex G-100 (Pharmacia Fine Chemicals, Uppsala, Sweden) column chromatography and filtration. Emulsions were separated from free paclitaxel in the Sephadex G-100 column using a mobile phase of 5% glucose solution. The amounts of paclitaxel in the free fraction and the emulsion fraction were determined by HPLC as described in the "HPLC" section. With the other method, the emulsions were filtrated through 0.45-μm Ekikrodisc and the concentration of paclitaxel in the filtrate was determined by HPLC. It was found that the amount of paclitaxel determined by the two methods was the same in the preliminary experiment. So the simpler method of filtration was selected in this study.

The entrapment efficiency was calculated according to the following equation:

$$\text{Entrapment efficiency (\%)} = (A_e/A_t) \times 100$$

where A_e is the amount of paclitaxel detected in the emulsion form and A_t is the total amount of paclitaxel added.

Stability

After their preparation, paclitaxel emulsions were stored at 4°C in the dark for 10 days. The stability was assessed by monitoring the changes in the particle size and paclitaxel content of emulsions during the storage period, which were calculated using the following equations:

$$\text{Change of particle size (\%)} = (S_{10}/S_0) \times 100$$

where S_{10} was the size on the tenth day and S_0 was the size on the day of preparation;

$$\text{Change of drug concentration (\%)} = (C_{10}/C_0) \times 100$$

where C_{10} was the concentration in the emulsion form on the tenth day and C_0 was the concentration in the emulsion form on the day of preparation. The paclitaxel concentration was determined by the HPLC method.

Experimental Design and Data Analysis

The amounts of soybean oil (X1), PEG-DSPE (X2), and polysorbate 80 (X3) were selected as causal factors in this study. The values listed in Table I in coded form were transformed to physical units as summarized in Table II. A spherical experimental design for three factors was used to prepare the model formulations (Nos. 1–15). The response of the experimental design was adapted to particle size, entrapment efficiency and stability of paclitaxel emulsions on the tenth day.

The software ANN and ALCORA were used to analyze the results of the experiment (25,27). Levels of causal factors were expressed as concentrations (mg/ml).

RESULTS AND DISCUSSION

In this study, a Cremophor-free oil-in-water emulsion of paclitaxel was developed using all excipients, which are less toxic and present in a number of marketed parenteral products. In a preliminary experiment, the particle size and amount of paclitaxel in the emulsion were measured after storage at 4°C for 1 month using oleic acid, vitamin E and soybean oil as an internal phase and polysorbate 80, PEG-

Table I. Spherical (Nos. 1–15) Experimental Design for Three Factors

Formulation no.	X_1	X_2	X_3
1	−1	−1	−1
2	−1	−1	1
3	−1	1	−1
4	−1	1	1
5	1	−1	−1
6	1	−1	1
7	1	1	−1
8	1	1	1
9	−1.73	0	0
10	1.73	0	0
11	0	−1.73	0
12	0	1.73	0
13	0	0	−1.73
14	0	0	1.73
15	0	0	0

DSPE and cholesterol as emulsifiers or co-emulsifiers with a paclitaxel concentration of 0.3 to 1.8 mg/ml. From the results, soybean oil as the oil phase and 0.3 mg/ml of paclitaxel were more stable than the others (data not shown). Therefore, soybean oil was used as the internal phase. Polysorbate 80 with a polyethylene glycol group chain, a surfactant in common use, was used to conduce a paclitaxel formulation. PEG-DSPE was supposed not only to prolong circulation time *in vivo* but also to form an injectable paclitaxel emulsion. Cholesterol was used to stabilize the surface of droplets together with PEG-DSPE (18). Therefore, cholesterol was used in the same amount (weight) as PEG-DSPE. In the formulations of emulsions of paclitaxel, constant amount of paclitaxel, PEG 400 and glucose (constant volume of 5% glucose solution) was added and the final volume of emulsion was adjusted same by drops of Milli Q water.

Spherical Experimental Design

The data of spherical design in the model formulation are listed in Table III, including particle size, entrapment efficiency and stability of paclitaxel emulsions on the tenth day. The data were called responses and marked as Y1 to Y4, respectively. A significant difference in the value of responses can be observed. The entrapment efficiency (Y1) was 79.2%~101.5%, particle size after preparation (Y2) was 256.6~348.5 nm, change of concentration (Y3) was 19.0~99.3% and change of particle size (Y4) was 79.6~106.6%.

ANN was applied to the prediction of responses (Y1–Y4) as a function of causal factors. 2PE was used for comparing the prediction ability.

Three causal factors corresponding to different levels of soybean oil (X1), PEG-DSPE (X2), and polysorbate 80 (X3)

Table II. Levels of Causal Factors* in Physical Form

	Factor level in coded form				
Factor	−1.73	−1	0	1	1.73
Soybean oil (X_1)	4.8	7	10	13	15.2
PEG-DSPE (X_2)	1.3	2	3	4	4.7
Polysorbate 80 (X_3)	15.2	24	36	48	56.8

* Levels of causal factors were expressed as concentrations (mg/ml).

Table III. Results of Experimental Design

	Y1* (%)	Y2† (nm)	Y3‡ (%)	Y4§ (%)
1	90.8 ± 0.5	276.2 ± 3.4	61.9 ± 1.6	99.7 ± 2.1
2	101.5 ± 0.2	277.6 ± 2.3	95.4 ± 2.6	90.4 ± 1.7
3	95.4 ± 1.9	295.3 ± 1.0	35.2 ± 1.3	83.4 ± 1.2
4	86.2 ± 0.9	283.1 ± 2.1	94.2 ± 1.8	94.9 ± 1.1
5	82.1 ± 1.4	328.8 ± 0.5	55.6 ± 2.6	83.9 ± 1.1
6	92.7 ± 1.0	325.0 ± 3.1	99.3 ± 2.9	91.6 ± 1.0
7	90.0 ± 1.0	289.1 ± 3.4	41.7 ± 1.3	79.6 ± 1.3
8	93.4 ± 0.7	335.0 ± 3.1	97.5 ± 2.1	90.2 ± 1.3
9	92.5 ± 1.5	256.6 ± 2.7	88.2 ± 0.1	106.6 ± 1.5
10	85.3 ± 1.6	314.8 ± 2.8	92.2 ± 2.5	93.8 ± 0.7
11	93.7 ± 0.1	348.5 ± 4.1	90.4 ± 1.6	96.4 ± 2.0
12	87.4 ± 2.6	275.0 ± 1.4	74.7 ± 3.6	104.4 ± 0.9
13	90.1 ± 0.4	268.7 ± 4.0	19.0 ± 0.3	93.1 ± 1.4
14	86.2 ± 0.7	291.1 ± 2.5	94.5 ± 2.0	103.4 ± 1.7
15	79.2 ± 0.8	260.5 ± 2.5	58.6 ± 1.2	105.5 ± 1.3

* Entrapment efficiency after preparation.
† Particle size after preparation.
‡ Change of concentration (10 day/0 day).
§ Change of particle size (10 day/0 day).

were used as each nod of the input layer. Reponses were predicted individually with the different sets of ANN. A set of causal factors and responses [45 data pairs; triplicate measurements for 15 formulations (Table I)] was used as tutorial data for ANN. To optimize the structure of ANN, the simulated annealing technique (30) was applied, employing AIC (Akaike's information criterion) as a standard (27). Results are shown in Table IV, suggesting that 4 or 5 nods in the hidden layers were optimal for the prediction of responses, Y1 and Y3, or Y2, and Y4. This means 16 or 20 unknown parameters (3 input nods, 4 or 5 hidden nods, and 1 output nod; i.e., 3×4 + 4×1 = 16 or 3×5 + 5×1 = 20) were required to fit the weights of ANN for the prediction of responses. On the other hand, 2PE requires an estimation of 10 unknown parameters at most as regression coefficients of the polynomial equation [i.e., 3 parameters for the independent term (X1, X2, and X3), 3 for the square term (X1X1, X2X2, and X3X3), 3 for the interaction term (X1X2, X1X3, and X2X3), and 1 for the constant]. To enable an impartial comparison of the predictive ability of ANN and 2PE, we used the coefficient of determination, which was doubly adjusted with degrees of freedom (R**2). As a result, predicted values of

Table IV. Optimal Structures of ANN for Prediction of Responses

Response	Y1	Y2	Y3	Y4
Optimal ANN*	3/4/1	3/5/1	3/4/1	3/5/1
R†	0.984	0.977	0.999	0.991
R**2‡	0.933	0.881	0.996	0.953
AIC§	−80.8	−128	−180	−84.2

* Optimal structure of ANN; input nods/hidden nods/output nods.
† Multiple correlation coefficient between predicted and experimental response values.
‡ Coefficient of determination doubly adjusted with degrees of freedom.
§ Akaike's information criterion. Smaller values of AIC mean a better approximation. The structure of ANN, which gives the smallest value of AIC, was chosen as the optimum.

Table V. Comparisons of Prediction with Results of Experiments

	Y1 (%)	Y2 (nm)	Y3 (%)	Y4 (%)
ANNp*	101	262	96.2	99.7
ANNr†	96.7	262	97.6	98.1
2PEp‡	95.1	267	95.3	97.8
2PEr§	92.6	358	100	88.1

* Predicted by ANN.
† Data of experiment with the optimal formulation predicted by ANN; X1 = 5.50, X2 = 2.18, X3 = 36.0 (mg/ml).
‡ Predicted by 2PE.
§ Data of experiment with the optimal formulation predicted by 2PE, X1 = 5.45, X2 = 2.18, X3 = 42.8 (mg/ml).

responses based on ANN coincided well with the experimental values (Table V). However, approximations of responses based on 2PE were somewhat poorer ($R = 0.895$ and $R^{**}2 = 0.702$ for Y1; $R = 0.900$ and $R^{**}2 = 0.714$ for Y2; $R = 0.977$ and $R^{**}2 = 0.973$ for Y3; $R = 0.783$ and $R^{**}2 = 0.335$ for Y4).

Entrapment Efficiency

The contribution indices (27) of the factors in the formulation were calculated by ANN and are summarized in Table VI. The larger the value is the more important the factor. The entrapment efficiency of 0.6 mg/ml paclitaxel after preparation (Y1) was affected in the order PEG-DSPE (X2) > polysorbate 80 (X3) > soybean oil (X1). The soybean oil was relatively less important to entrapment efficiency. The influence of the main factors of PEG-DSPE and polysorbate 80 on the entrapment efficiency is shown in Fig. 1A. It was evident that the entrapment efficiency changed with the amount and ratio of PEG-DSPE and polysorbate 80. The solubility of paclitaxel in soybean oil is not high. Therefore, this finding suggested that most of the paclitaxel might be situated in the surface layer of emulsion droplets due to interaction of the drug with the PEG chain of PEG-DSPE and polysorbate 80 (2–7).

Table VI. Contribution Indices (%) of Factors on the Response in ANN Approximation

	Y1	Y2	Y3	Y4
X1	22.2	32.6	25.3	32.1
X2	40.4	44.2	28.4	32.6
X3	37.5	23.2	46.3	36.2

Particle Size

The particle size after preparation (Y2) was influenced in the order PEG-DSPE (X2) > soybean oil (X1) > polysorbate 80 (X3) (Table VI). The response of particle size to PEG-DSPE and soybean oil is depicted in Fig. 1B. A medium amount (about 2.4 mg/ml PEG-DSPE and 8.96 mg/ml soybean oil) of PEG-DSPE produced small particles (about 269 nm) in the preparation without any homogenization and extrusion of membranes. This finding corresponded well with the result that PEG-DSPE incorporated into emulsions formed small (less than 150 nm) particles (18,19).

Stability

The change in concentration was affected mainly by polysorbate 80 (X3) rather than PEG-DSPE (X2) and soybean oil (X1). Polysorbate 80 (X3) was also important to the change in particle size (Y4) (Table VI). Figures 2A and 2B show the relationship between the two main factors and respective responses in terms of the experimental design. A large amount (>41 mg/ml) of polysorbate 80 and large (>4.4

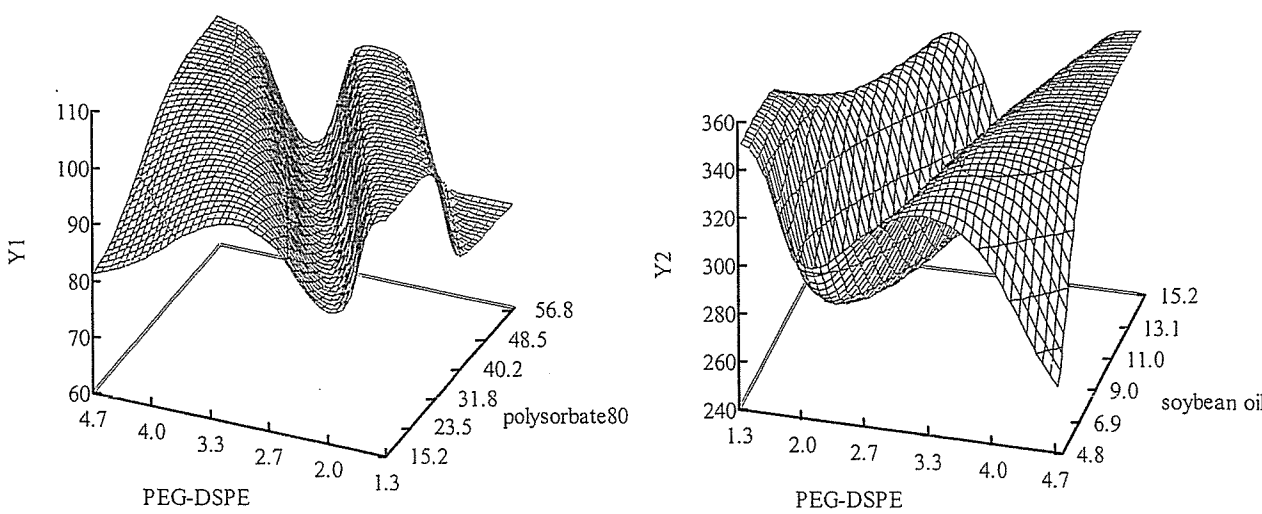

(A) (B)

Fig. 1. The effect of PEG-DSPE and polysorbate 80 (mg/ml) on the entrapment efficiency of paclitaxel emulsions (Y1) (A), and the effect of PEG-DSPE and soybean oil (mg/ml) on the particle size of paclitaxel emulsions (Y2) (B).

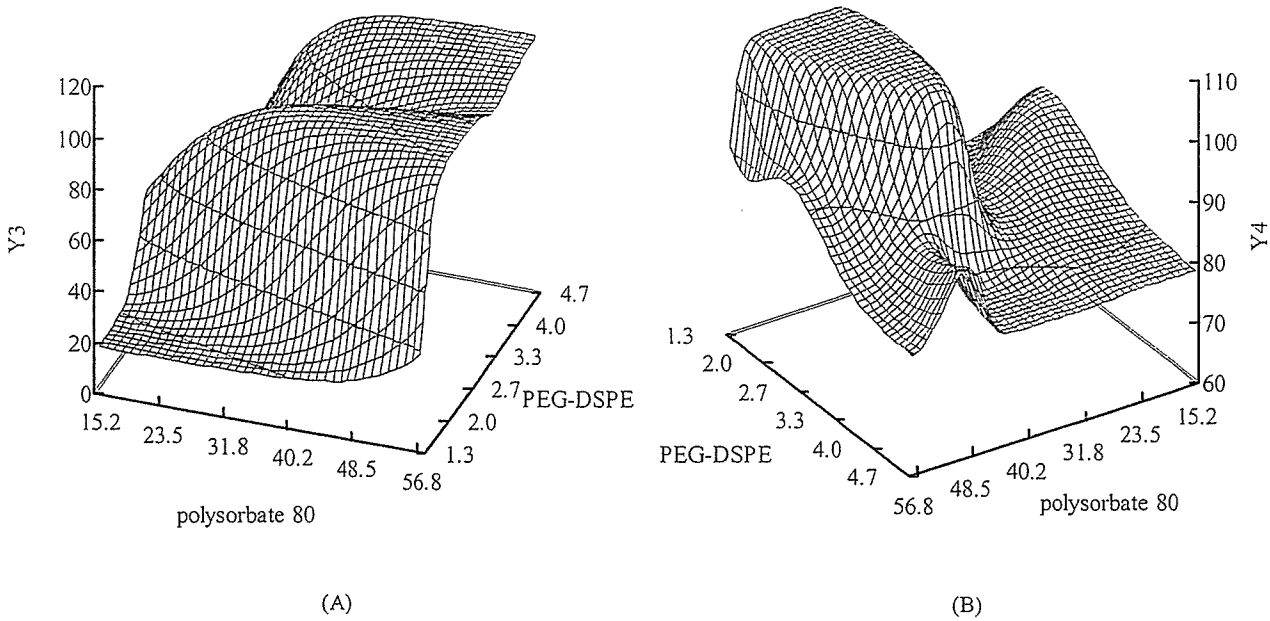

Fig. 2. The effect of polysorbate 80 and PEG-DSPE (mg/ml) on the change in the concentration of paclitaxel emulsions (Y3) (A), and particle size of paclitaxel emulsions (Y4) (B).

mg/ml) or medial (2.1~2.9 mg/ml) amount of PEG-DSPE brought about a more stable concentration of paclitaxel emulsions (Y3) (Fig. 2A), but a large amount (>39 mg/ml) of polysorbate 80 and small amount (<3.3 mg/ml) of PEG-DSPE led to a more stable particle size (Y4) (Fig. 2B). The results indicate that particles modified with a PEG chain proved more stable than those without modification (3).

In some formulations crystals could be observed after ten days and were proved to be paclitaxel by HPLC. And the products of hydrolysis of paclitaxel almost could not be detected by HPLC. Thus it was concluded that the decrease on concentration of paclitaxel was caused mainly by the release of paclitaxel from emulsions and the formation of crystals of paclitaxel in external phase.

Prediction of Optimal Formulation

The software ANN and ALCORA was used to predict the optimal formulation. Two optimal formulations of paclitaxel emulsions were prepared according to the results of predictions by ANN and ALCORA, respectively. The optimal formulations containing 0.6 mg/ml paclitaxel, 30 mg/ml PEG 400, and 50 mg/ml glucose were as follows: by ANN, 5.50 mg/ml soybean oil (X1), 2.18 mg/ml PEG-DSPE (X2), 36.0 mg/ml polysorbate 80 (X3); by 2PE, 5.45 mg/ml soybean oil (X1), 2.18 mg/ml PEG-DSPE (X2), 42.8 mg/ml polysorbate 80 (X3). Then the four parameters of entrapment efficiency after preparation (Y1), particle size after preparation (Y2), change of concentration on the tenth day (Y3) and change of particle size on the tenth day (Y4) were determined. The results are shown in Table V along with the predicted responses. Comparing the predictions and results of experiments, ANN was found to be more suitable for the formulation of paclitaxel emulsions.

Although a number of important formulation parameters remain to be optimized for clinical application, there is indication, at least in paclitaxel PEGylated emulsions, that polysorbate 80 is essential. This information is new with regard to paclitaxel emulsions. PEGylated microemulsions are expected to show long-circulating emulsions *in vivo*. Further research is needed to confirm the efficacy of paclitaxel emulsions *in vivo*.

CONCLUSIONS

We describe here a novel PEGylated emulsion formulation containing paclitaxel that has been optimized by spherical experimental design and ANN for small size (262 nm), high entrapment efficiency (96.7%), and stability. Paclitaxel emulsions were prepared using a very simple procedure and commercialized components for replacement of the toxic Cremophor EL. The contribution indices of each component suggested that PEG-DSPE mainly contributes to the entrapment efficiency and particle size, while polysorbate 80 contributes to the stability of paclitaxel emulsions.

ACKNOWLEDGMENTS

This project was supported in part by a grant from The Promotion and Mutual Aid Corporation for Private Schools of Japan and by a Grant-in-Aid for Scientific Research from the Ministry of Education, Culture, Sports, Science, and Technology of Japan. This work was also supported by Hoshi University. There has been a sister-relationship between Hoshi University and the School of Pharmaceutical Sciences, Peking University.

REFERENCES

1. A. K. Singla, A. Garg, and D. Aggarwal. Paclitaxel and its formulation. *Int. J. Pharm.* **235**:179–192 (2002).
2. B. D. Tarr, T. G. Sambandan, and S. H. Yalkowsky. A new

paranteral emulsion for the administration of taxol. *Pharm. Res.* **4**:162–165 (1987).
3. J. J. Wheeler, K. F. Wong, S. M. Ansell, D. Masin, and M. B. Bally. Polyethlene glycol modified phospholipids stabilize emulsions prepared from triacylglycerol. *J. Pharm. Sci.* **83**:1558–1564 (1994).
4. B. B. J. Lunberg. A submicron lipid emulsion coated with amphipathic polyethylene glycol for parenteral administration of paclitaxel (taxol). *Pharm. Pharmacol.* **49**:16–21 (1997).
5. P. Kan, Z. B. Chen, C. J. Lee, and I. M. Chu. Development of nonionic surfactant/phospholipid/ o/w emulsion as a paclitaxel delivery system. *J. Control. Rel.* **58**:271–278 (1999).
6. P. Simamora, R. M. Dannenfelser, S. E. Tabibi, and S. H. Yalkowsky. Emulsion formulation for intravenous administration of paclitaxel. *PDA J. Pharm. Tech.* **52**:170–172 (1998).
7. P. P. Constantinides, K. J. Lambert, A. K. Tustian, B. Schneider, S. Lalji, W. Ma, B. Wentzel, D. Kessler, D. Worah, and S. C. Quay. Formulation development and antitumor activity of a filter-sterilizable emulsion of paclitaxel. *Pharm. Res.* **17**:175–182 (2000).
8. R. T. Liggins and H. M. Burt. Paclitaxel loaded poly (L-lactic acid) microspheres: properties of microspheres made with low molecular weight polymers. *Int. J. Pharm.* **222**:19–33 (2001).
9. L. Mu and S. S. Feng. Vitamin E TPGS used as emulsifier in the solvent evaporation/extraction technique for fabrication of polymeric nanospheres for controlled release of paclitaxel (Taxol®). *J. Control. Rel.* **80**:129–144 (2002).
10. P. Crosasso, M. Ceruti, P. Brusa, S. Arpicco, F. Dosio, and L. Cattel. Preparation, characterization and properties of sterically stabilized paclitaxel-containing liposomes. *J. Control. Rel.* **63**:19–30 (2000).
11. N. V. Koshkina, J. C. Waldrep, L. E. Roberts, E. Golunski, S. Melton, and V. Knight. Paclitaxel liposome aerosol treatment induces inhibition of pulmonary metastases in murine renal carcinoma model. *Clin. Cancer Res.* **7**:3258–3262 (2001).
12. S. C. Kim, D. W. Kim, Y. H. Shim, J. S. Bang, H. S. Oh, S. W. Kim, and M. H. Seo. In vivo evaluation of polymeric micellar paclitaxel formulation: toxicity and efficacy. *J. Control. Rel.* **72**: 191–202 (2001).
13. A. Miwa, A. Ishibe, M. Nakano, T. Yamahira, S. Itai, S. Jinno, and H. Kawahara. Development of novel chitosan derivatives as micellar carriers of taxol. *Pharm. Res.* **15**:1844–1850 (1998).
14. S. Alcaro, C. A. Ventura, D. Paolino, D. Battaglia, F. Ortuso, L. Cattel, G. Puglisi, and M. Fresta. Preparation, characterization, molecular modeling and in vitro activity of paclitaxel-cyclodextrin complexes. *Bioorg. Med. Chem. Lett.* **12**:1637–1641 (2002).
15. H. Kim, J. Choi, H. W. Kim, and S. Jung. Monte Carlo docking simulations of cyclomaltoheptaose and dimethyl cyclomaltoheptaose with paclitaxel. *Carbohydr. Res.* **337**:549–555 (2002).
16. F. Dosio, S. Arpicco, P. Brusa, B. Stella, and L. Cattel. Poly (ethylene glycol)-human serum albumin-paclitaxel conjugates: preparation, characterization and pharmacokinetics. *J. Control. Rel.* **76**:107–117 (2001).
17. G. M. Zentner, R. Rathi, C. Shih, and J. C. McRea. M H. Seo, H. Oh, B. G. Rhee, J. Mestecky, Z. Moldoveanu, M. Morgan, and S. Weitman. Biodegradable block copolymers for delivery of proteins and water-insoluble drugs. *J. Control. Rel.* **72**:203–215 (2001).
18. J. Wang, Y. Maitani, and K. Takayama. Antitumor effects and pharmacokinetics of aclacinomycin A carried by injectable emulsions composed of vitamin E, cholesterol and PEG-lipid. *J. Pharm. Sci.* **91**:1128–1134 (2002).
19. J. Wang, K. Takayama, T. Nagai, and Y. Maitani. Pharmacokinetics and antitumor effects of vincristine carried by microemulsions composed of and PEG-lipid, oleic acid, vitamin E and cholesterol. *Int. J. Pharm.* **251**:13–21 (2003).
20. A. S. Hassian and R. D. Johnson. Application of neural computing in pharmaceutical product development. *Pharm. Res.* **8**:1248–1252 (1991).
21. A. S. Hussain, R. D. Johnson, N. Vachharajani, and W. A. Ritschel. Feasibility of developing a neural network for prediction of human pharmacokinetic parameters from animal data. *Pharm. Res.* **10**:466–469 (1993).
22. B. P. Smith and M. E. Brier. Statistical approach to neural network model building for gentamicin peak prediction. *J. Pharm. Sci.* **85**:65–99 (1996).
23. A. S. Achanta, J. G. Kowalski, and C. T. Rhodes. Artificial neural networks: Implications for pharmaceutical sciences. *Drug Dev. Ind. Pharm.* **21**:119–155 (1995).
24. K. Takayama and T. Nagai. Simultaneous optimization for several characteristics concerning percutaneous absorption and skin damage of ketoprofen hydrogels containing d-limonene. *Int. J. Pharm.* **74**:115–126 (1991).
25. J. Takahara, K. Takayama, K. Isowa, and T. Nagai. Multi-objective simultaneous optimization based on artificial neural network in a ketoprofen hydrogel formula containing O-ethylmenthol as a percutaneous absorption enhancer. *Int. J. Pharm.* **158**:203–210 (1997).
26. K. Takayama, M. Fujikawa, and T. Nagai. Artificial neural network a novel method to optimize pharmaceutical formulations. *Pharm. Res.* **16**:1–6 (1999).
27. P. C. Wu, Y. Obata, M. Fijikawa, C. J. Li, K. Higashiyama, and K. Takayama. Simultaneous optimization based on artificial neural networks in ketoprofen hydrogel formula containing o-ethyl-3-butylcyclohexanol as percutaneous absorption enhancer. *J. Pharm. Sci.* **90**:1004–1013 (2001).
28. S. Batzri and E. D. Korn. Single bilayer liposomes prepared without sonication. *Biophys. Acta* **298**:1015–1019 (1973).
29. S. H. Lee and S. D. Yoo and K. H Lee. Rapid and sensitive determination of paclitaxel in mouse plasma by high-performance liquid chromatography. *J. Chromatogr. B* **724**:357–363 (1999).
30. S. Kirkpatrick, C. D. Gelatt, and M. P. Vecchi. Optimization by simulated annealing. *Science* **200**:671–680 (1983).

Journal of Drug Targeting, July 2004 Vol. 12 (6), pp. 373–384

Taylor & Francis
healthsciences

Polymer Design and Incorporation Methods for Polymeric Micelle Carrier System Containing Water-insoluble Anti-cancer Agent Camptothecin

MASAYUKI YOKOYAMA[a], PRANEET OPANASOPIT[a], TERUO OKANO[a,*], KUMI KAWANO[b] and YOSHIE MAITANI[c]

[a]*Institute of Advanced Biomedical Engineering and Science, Tokyo Women's Medical University, Kawada-cho 8-1, Shinjuku-ku, Tokyo 162-8666, Japan;* [b]*Institute of Medicinal Chemistry, Hoshi University, Ebara 2-4-41, Shinagawa-ku, Tokyo 142-8501, Japan;* [c]*Kanagawa Academy of Science and Technology, KSP East 404, Sakado 3-2-1, Takatsu-ku, Kawasaki-shi, Kanagawa-ken 231-0012, Japan*

A water-insoluble anti-cancer agent, camptothecin (CPT) was incorporated to a polymeric micelle carrier system forming from poly(ethylene glycol)–poly(aspartate) block copolymers. Incorporation efficiency and stability were analyzed in correlation with chemical structures of the inner core-forming hydrophobic blocks as well as with incorporation methods. Among three incorporation methods (dialysis, emulsion and evaporation methods), an evaporation method brought about much higher CPT yields with less aggregation than the other two methods. By the evaporation method, CPT was incorporated to polymeric micelles in considerably high yields and with high stability using block copolymers possessing high contents of benzyl and methylnaphtyl ester groups as hydrophobic moieties. This indicates importance of molecular design of the hydrophobic block chain to obtain targeting using polymeric micelle carriers as well as importance of the drug incorporation method.

Keywords: Polymeric micelle; Camptothecin; Block copolymer; Poly (ethylene glycol); Poly (aspartic acid); Targeting

Abbreviations: PEG, poly(ethylene glycol); P(Asp), poly(aspartic acid); PEG–P(Asp), poly(ethylene glycol)–poly(aspartic acid) block copolymer; PEG–PBLA, poly(ethylene oxide)–poly(β-benzyl L-aspartate) block copolymer; CPT, camptothecin; DMSO, dimethyl sulfoxide; DMF, N,N-dimethylformamide; DBU, 1,8-diazabicyclo [5,4,0] 7-undecene

INTRODUCTION

Polymeric micelles attract much attention as a nano-sized drug carrier system (Kwon and Kataoka, 1995; Kabanov and Alakhov, 1997; Yokoyama, 1998, 2002; Kwon and Okano, 1999; Lavasanifar *et al.*, 2002 and Nishiyama and Kataoka 2003) due to their advantageous characteristics for drug targeting such as very small size in a range of 10–100 nm and high structural stability. Particularly, two advantages are significant for anti-cancer drug targeting to solid tumors; passive targeting ability to solid tumors and applicability to water-insoluble drugs. Polymeric micelles can be delivered selectively to solid tumor sites by a passive targeting mechanism based on the enhanced permeability and retention effect (EPR effect) (Matsumura and Maeda, 1986; Maeda, 2000; Maeda *et al.*, 2002). Long-circulation in the bloodstream is a prerequisite for the EPR effect in order to evade non-selective scavenge at the reticuloendothelial system. Hydrophobic (Illum *et al.*, 1987) and cationic (Takakura and Hashida, 1996) characters of anti-cancer drugs are a promotion factor of this scavenge and can be a serious problem of drug-polymer conjugates because the conjugated drugs are exposed to interact with biocomponents such as proteins and cells. For polymeric micelles, the drug-incorporated inner core is clearly separated from the hydrophilic outer shell that is responsible for interactions with the biocomponents. Therefore, polymeric micelles can attain the long-circulation in the bloodstream (Yokoyama *et al.*, 1991; Kwon *et al.*, 1993) while incorporating a large amount of anti-cancer drugs with cationic and/or hydrophobic characters such as doxorubicin.

The second advantage for solid tumor targeting is excellent applicability to hardly water-soluble or water-insoluble anti-cancer drugs. Since many recently developed potent anticancer drugs such as taxol, camptothecin (CPT) and iressa are water-insoluble, applicability of drug carrier systems to the water-insoluble drug is important. One of the most successful types of drug carriers is a liposome that consists of a lipid bilayer

*Corresponding author. Tel.: +81-3-3353-8111. Ext. 30233. Fax: +81-3-3359-6046. E-mail: tokano@abmes.twmu.ac.jp

ISSN 1061-186X print/ISSN 1029-2330 online © 2004 Taylor & Francis Ltd
DOI: 10.1080/10611860412331285251

and an interior aqueous phase which is surrounded by the lipid bilayer. A famous successful example of liposomal carrier systems is Doxil™ that incorporates doxorubicin for tumor targeting. Liposomal carrier systems are favorable for incorporation of hydrophilic and water-soluble drugs in their interior aqueous phase, however, their applications are considerably limited for hydrophobic and water-insoluble drugs because these hydrophobic drugs are loaded in lipid bilayers, not in an interior aqueous phase. It is considered difficult to maintain good targeting properties of the bilayer when this bilayer is loaded with a large amount of the drug. For polymeric micelle systems, a large amount of water-insoluble drug can be incorporated to the hydrophobic inner core with maintaining good properties for targeting owing to the distinctly separated two-phase structure of the hydrophobic inner core and the hydrophilic outer shell.

Anti-cancer drug targeting using polymeric micelle carrier systems was first achieved with doxorubicin (adriamycin) (Yokoyama *et al.*, 1987; Yokoyama *et al.*, 1990; Yokoyama *et al.*, 1991; Yokoyama *et al.*, 1998; Yokoyama *et al.*, 1999). Doxorubicin was conjugated to aspartic acid residues of poly(ethylene glycol)-poly(aspartic acid) block copolymer. This doxorubicin-block copolymer conjugate formed a micellar structure due to its amphiphilic character of the hydrophilic poly(ethylene glycol) block and the hydrophobic doxorubicin-conjugated poly(aspartic acid) block. Furthermore, Doxorubicin was incorporated in the hydrophobic inner core by physical entrapment, and was targeted to solid tumor sites with high selectivity. As a result of this targeting, dramatically enhanced *in vivo* anti-tumor effects were obtained (Yokoyama *et al.*, 1999). This doxorubicin polymeric micelle system is now in the phase II clinical trail starting in autumn of 2003 at the National Cancer Hospital, Japan. In this system, doxorubicin was chemically conjugated to the aspartic acid residue of the block copolymer and this conjugated doxorubicin worked as a hydrophobic species for micelle formation and physical incorporation of further doxorubicin molecules (Yokoyama *et al.*, 1998). This physically incorporated doxorubicin expressed selective anticancer activity by being targeted to solid tumor sites (Yokoyama *et al.*, 1998, 1999). Therefore, the chemically conjugated doxorubicin did not play a role of anticancer effect. It is preferable to design targeting systems without using drug molecules as a biologically inactive hydrophobic species to suppress production cost as well as to allow much wider choice for the hydrophobic species. The wider choice of simpler hydrophobic chemical structures (e.g. phenyl ring and acyl chain) than drug molecules is considered to be very advantageous for optimization of the influencing factors for targeting (e.g. micelle stability, size and drug release rate).

On the other hand, applications of the polymeric micelle carrier systems to other anti-cancer drugs are now actively studied with various drugs such as cisplatin (Nishiyama *et al.*, 1999; Nishiyama and Kataoka, 2003), taxol, methotrexate (Li and Kwon, 2000) and KRN-5500 (Matsumura *et al.*, 1999; Mizumura *et al.*, 2002). For water-insoluble anti-tumor drugs such as taxol and KRN-5500, the drug incorporation is clinically beneficial in evasion of the use of toxic substances that dissolve these water-insoluble drugs for intravenous injection. This is exemplified by cremophor EL and ethanol used to dissolve taxol in an aqueous medium. Since polymeric micelles are generally much less toxic than these substances, the drug solubilization by incorporation to polymeric micelles can decrease toxic side effects that result from these substances. In fact, incorporation of KRN-5500 to polymeric micelles diminished vascular and pulmonary toxicities resulting from organic solvents and surfactants that were used in a conventional formulation (Matsumura *et al.*, 1999; Mizumura *et al.*, 2002). However, targeting of KRN-5500 to tumors has not yet been done. In this paper, block copolymer syntheses and drug incorporation to polymeric micelles are reported for targeting of CPT (Potmesil, 1994; Wall and Wani, 1995a, b) that is a mother compound of topotecan and CPT-11, which are very potent and recently approved as anticancer-drugs.

For tumor targeting with the polymeric micelles, several physical and physico-chemical factors were known to be important such as block length (Kwon *et al.*, 1993; Yokoyama *et al.*, 1993) and drug content (Yokoyama *et al.*, 1998). Even though chemical structures of the inner core-forming block were partially examined for tumor targeting (Yokoyama *et al.*, 1998), no systematic study has been done to establish a strategy of polymeric micelle design for various kinds of anti-cancer drugs without using drug itself as a hydrophobic species for micelle formation and drug incorporation as done in the doxorubicin system (Yokoyama *et al.*, 1998, 1999). For polymeric micelle design, influencing factors on targeting may be hydrophobic strength, rigidity/flexibility, $\pi-\pi$ interactions (cohesive interactions between π electron rich molecules like benzene) of the hydrophobic inner core, block lengths of polymers and drug contents as well as steric space in the hydrophobic block for drug incorporation. This study aims to reveal correlations between these factors and drug targeting. Additionally, only a little study has been done for optimization of drug incorporation procedures to polymeric micelles (Kwon *et al.*, 1994; Kohori *et al.*, 2002). This study also aims to analyze effects of drug incorporation methods.

In this paper, various poly(ethylene glycol)–poly (aspartate ester) block copolymers were synthesized by varying chemical structures of hydrophobic ester groups and their incorporation behaviors (loading efficiency and incorporation stability) of CPT were systemically analyzed by three incorporation methods.

MATERIALS AND METHODS

Chemicals

(s)-(+)-CPT was purchased from Aldrich Chem. Co., Milw., WI, USA. 1,8-Diazabicyclo [5,4,0] 7-undecene